Mon. Not. R. astr. Soc. (1988) **231,** 1077–1090

Spectrophotometric and neutral hydrogen observations of Michigan 160

D. J. Axon[1], L. Staveley-Smith[1]*, R. A. E. Fosbury[2]†, J. Danziger[3], A. Boksenberg[4] and R. D. Davies[1]

[1] *University of Manchester, Nuffield Radio Astronomy Laboratories, Jodrell Bank, Macclesfield, Cheshire SK11 9DL*

[2] *Space-Telescope European Coordinating Facility, European Southern Observatory, Karl Schwarzschild Str. 2, D-8046, Garching bei München, Federal Republic of Germany*

[3] *European Southern Observatory, Karl Schwarzschild Str. 2, D-8046, Garching bei München, Federal Republic of Germany*

[4] *Royal Greenwich Observatory, Herstmonceux Castle, Hailsham, East Sussex BN27 1RP*

Accepted 1987 October 30; Received 1987 September 29

Summary. Spectrophotometry, deep optical imagery and neutral hydrogen observations of the emission-line galaxy Michigan 160 are presented. It is identified as a young, gas-rich system dominated by four massive H II regions. The galaxy has a disturbed optical structure suggestive of recent interaction, and it is probable that its neutral gas content (which exceeds 50 per cent of its total mass) is truly primordial. The metallicities and neutral gas fractions for Michigan 160 and a sample of similar emission-line and late-type galaxies are adequately explained by a chemical evolution model in which (i) the heavy element yield is constant (p=0.004) and (ii) the enrichment process is modified by inflow.

1 Introduction

Attention was first drawn to Michigan 160 (=UGC 12578) as an extragalactic emission-line object by MacAlpine, Smith & Lewis (1977), who used the Curtis Schmidt telescope at Cerro Tololo in combination with a thin objective prism. On Palomar Sky Survey prints it appears as a series of four bright condensations, aligned in an east–west direction and embedded in a nebulous halo of low surface brightness about 40 arcsec in diameter. This structure, coupled with its low luminosity (and probable low mass), suggested to us that Michigan 160 was either a member of the class of objects widely referred to as 'isolated extragalactic H II regions' (henceforth IEHRs) or an irregular galaxy undergoing a large burst of star formation. The early work by Sargent & Searle

* Present address: Anglo-Australian Observatory, PO Box 296, Epping, NSW 2121, Australia.
† Affiliated to the Astrophysics Division, Space Science Department, European Space Agency.

(1970) on the archetypal IEHRs, IZw18 and IIZw40, demonstrated their potential as a source of information on the enrichment process of the heavy elements in galaxies. Such systems have become the subject of intensive observational and theoretical study (Pagel & Edmunds 1981, and references therein), as they provide a simple environment for studying the relationship between star formation and chemical evolution, and currently provide the most reliable estimates of the primordial helium abundance (Davidson & Kinman 1985). It is now generally accepted that the very low metal abundances which characterize IEHRs can only be produced if they are either truly young objects in which we are witnessing the very first stages of star formation, or older galaxies in which star formation is confined to energetic episodic bursts. The outstanding questions are which, if either, of these alternatives is correct, and what mechanism generated the star bursts? At the present stage of our understanding it seems essential to proceed in two ways. First, we can probe for old stellar populations in IEHRs using infrared photometry and spectroscopy (e.g. Thuan 1983; Gondhalekar *et al.* 1984), and secondly, we can obtain high-resolution images to search for morphological evidence which might tell us if 'external fuelling' due to either secondary infall or tidal interactions are prime agents in triggering the starbursts. Here we report the results of a spectrophotometric, H I and morphological study of one such system, Michigan 160. Our results suggest that Michigan 160 possesses a large reservoir of unprocessed gas at large radii suitable for fuelling the current burst of star formation which is occurring in the galaxy.

2 Observations

2.1 DIRECT PHOTOGRAPHY

A direct plate of Michigan 160 (Plate 1a) was obtained in 1-arcsec seeing at the prime focus of the 3.9-m Anglo-Australian Telescope under the auspices of the service photography scheme. The emulsion was hypersensitized IIIaJ in combination with a GG 385 filter, and the exposure time was 80 min. The four bright H II regions discussed above have been identified with the numbers 1–4, and with the exception of no. 1 are not resolved. Several other fainter H II regions are also visible in the centre of the galaxy and there is evidence for two disturbed arms emanating from the eastern end of the main body of the galaxy. The second brightest H II region, No. 4, is located on the projection of the most prominent of these features. The overall structure of the galaxy is more clearly shown in Plate 1(b), which is a photographically enhanced copy of Plate 1(a), kindly prepared for us by David Malin. It is now obvious that the galaxy is a highly disturbed system, the overall structure being reminiscent of magellanic irregulars like NGC 4449 and 1569. The angular extent of the outer envelope of the galaxy is 60×102 arcsec^2. At the distance of $57.3\,h_{50}^{-1}$ Mpc obtained below, this corresponds to linear dimensions of 28×17 kpc^2 (1 arcsecond=278 pc). The fuzzy patch 80 arcsec north of Michigan 160 (marked e in Plate 1b) is recognizable as a possible dwarf companion.

2.2 SPECTROPHOTOMETRY

Long-slit spectra of the four brightest H II regions were obtained at resolutions (FWHM) of 1.5 and 5 Å, in 1978 August, using the University College London Image Photon Counting System (IPCS, Boksenberg 1972) in conjunction with the Boller & Chivens spectrograph, mounted at the Cassegrain focus of the 3.6-m ESO telescope at La Silla. Two different slit settings were used, to give optimum coverage of the four regions, details of the observational parameters being given in Table 1. Fig. 1 illustrates the low-dispersion spectra of regions 1–4 in Michigan 160 between 3600 and 7100 Å. Intermediate dispersion spectra for region 4 are shown in Fig. 2. All the data were

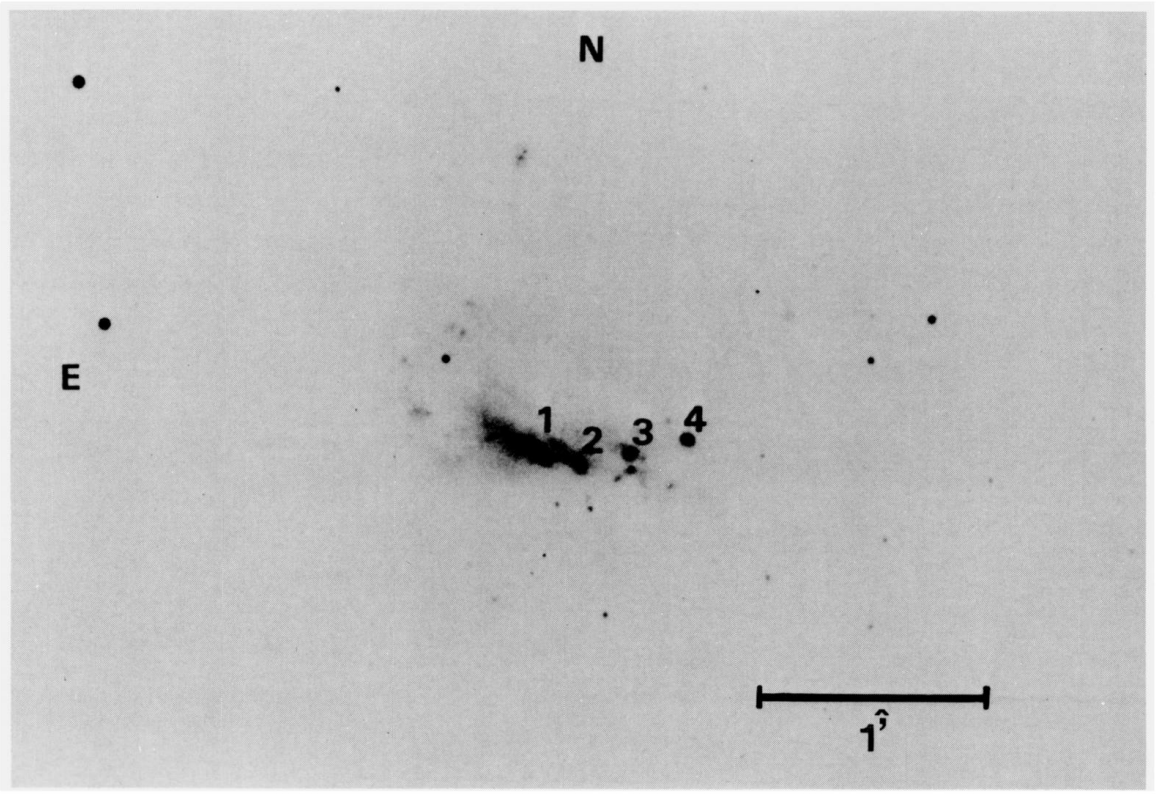

(a)

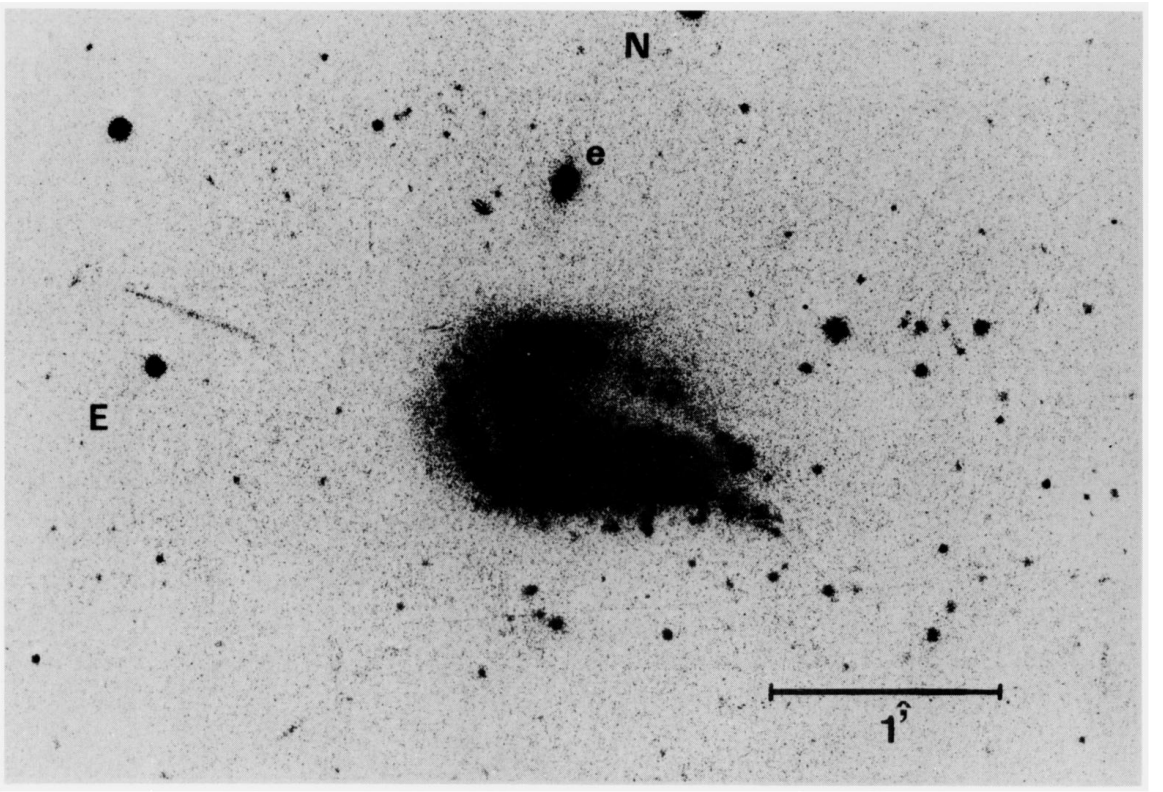

(b)

Plate 1. (a) Prime-focus plate of Michigan 160 taken with the 3.9-m Anglo-Australian Telescope. The seeing is 1 arcsec and the exposure time is 80 min. (b) Photographically enhanced version of (a) showing the disturbed outer arm structure in more detail. The object marked e is a dwarf companion.

[*facing page* 1078]

Table 1. Journal of spectroscopic observations.

ID	Objects	pa (°)	Resolution (Å)	Pixel Size (arcsec)	Slit width μm	Integration (sec)	Wavelength range (Å)	Comments
146/15	1,3,4	279	1.5	2.5	280	1800	3700–4500	
144/30	1,3,4	279	5	1.8	350	600	3500–6900	Seeing 2"
144/31	2,3	279	5	1.8	350	1320	3500–6900	
145/51	1,3,4	280	5.4	2.5	1000	1200	4250–5300	Wide slit
145/49	1,4	280	1.5	2.5	280	600	4250–5300	
141/63	1,4	279	1.5	2.5	280	1800	5800–7200	Cloud

analysed using the wavelength calibration and line profile fitting methods discussed by Axon & Taylor (1984). Flux calibration was achieved in a two-stage process. First, the emission-line fluxes of regions 2 and 3 were obtained using the wide (7 arcsec) slit observation in conjunction with observations of the photometric standard stars L749B, VMA2 and L870/2 (Oke 1974). We excluded [O III] λ5007 from this procedure, since in the wide-slit observations the counting rate was above the 10 per cent coincidence loss point for the IPCS. These results were then used to correct the narrow-slit data (obtained in an identical manner) assuming comparable slit losses for each region. Since the spectra were in general not obtained with the slit orientated along the parallactic angle, the line ratios obtained from the low-dispersion data are more susceptible to errors caused by atmospheric dispersion. The average values of the line strengths were therefore calculated from the low- and intermediate-dispersion data, giving twice the weight to the intermediate-dispersion data which have a higher signal-to-noise ratio. Table 2 lists the resulting logarithmic line strengths relative to Hβ, corrected for interstellar reddening computed from the observed and theoretical (Brocklehurst 1971) Balmer decrements together with the Whitford (1958) reddening law. All line strengths have been derived as the integral under the Gaussian curve fitted to each line. The computed value of $E(B-V)$ for each region is given. Also given in Table 2 are the absolute flux values of Hβ uncorrected for reddening, and the equivalent widths. Note that, since region 1 is appreciably extended compared to the other regions, the values obtained refer only to the core.

Radial velocities were derived from the weighted average of the stronger emission lines in the intermediate resolution spectra in the Hβ–[O III] 5007 region of the spectrum. At our resolution the lines in Michigan 160 are only marginally resolved. The resulting heliocentric velocities and line widths (corrected for instrumental resolution by making the reasonable approximation that both the instrumental and H II profiles are Gaussian) are again given for each region in Table 2. These results show that there is no appreciable velocity gradient ($\lesssim$25 km s^{-1}) across the H II regions, a point we will return to in view of the H I results below.

2.2 NEUTRAL HYDROGEN

Neutral hydrogen observations were made with the 76-m Lovell Telescope at Jodrell Bank which has a beamwidth of 12 arcmin at λ21 cm. Michigan 160 was observed on three separate occasions, on 1985 August 14 and 17 and on 1986 July 19. A system noise temperature of approximately 45 K was measured for each polarization channel on these occasions. The velocity resolution (FWHM) of the observations was 7 km s^{-1}. The average H I spectrum obtained from a total integration time

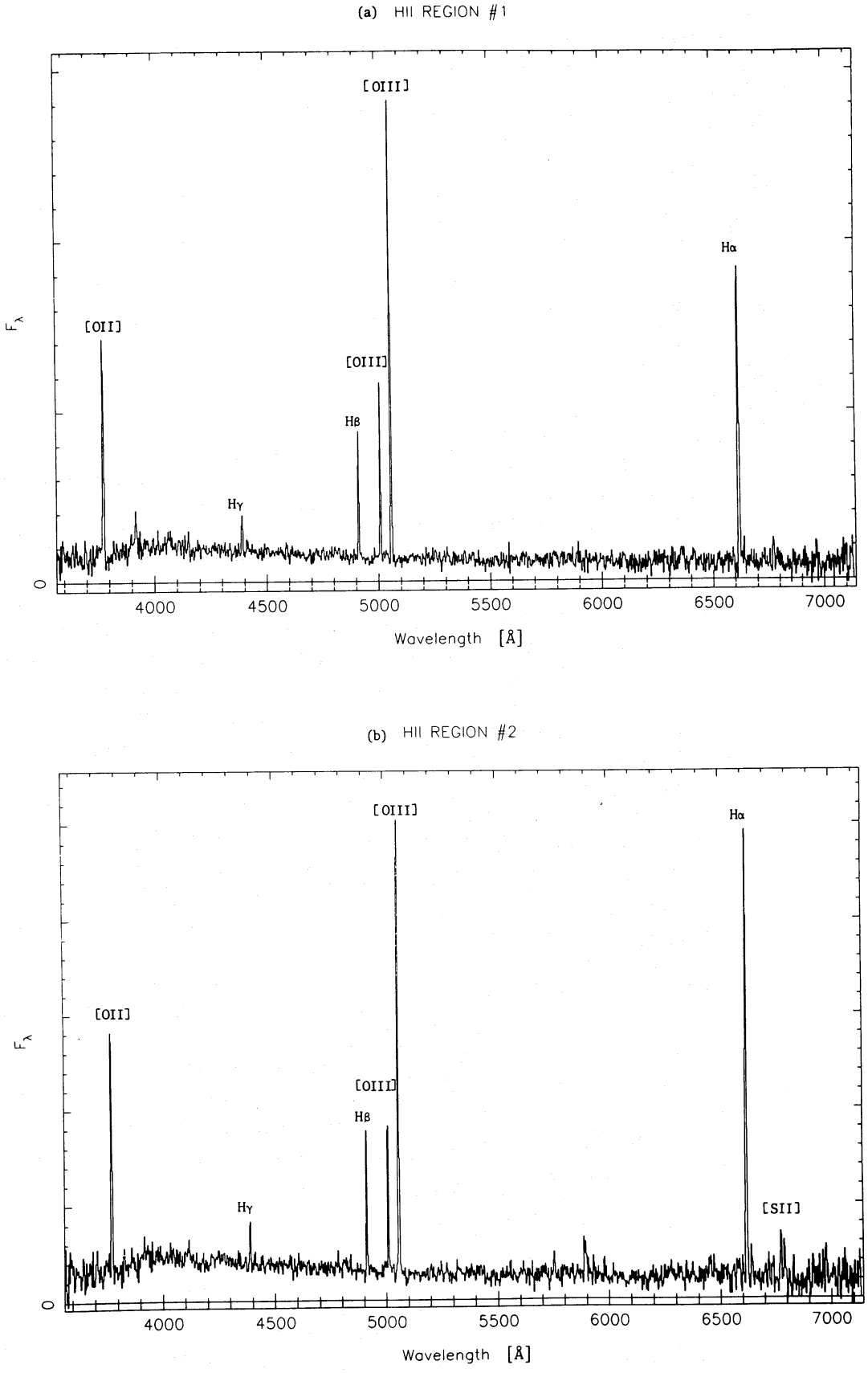

Figure 1. Low-dispersion spectra of regions 1–4 taken with the 3.6-m ESO telescope at La Silla. Exposure times are about 10 min and the resolution is 5 Å. F_λ is the flux per Ångström (arbitrary units).

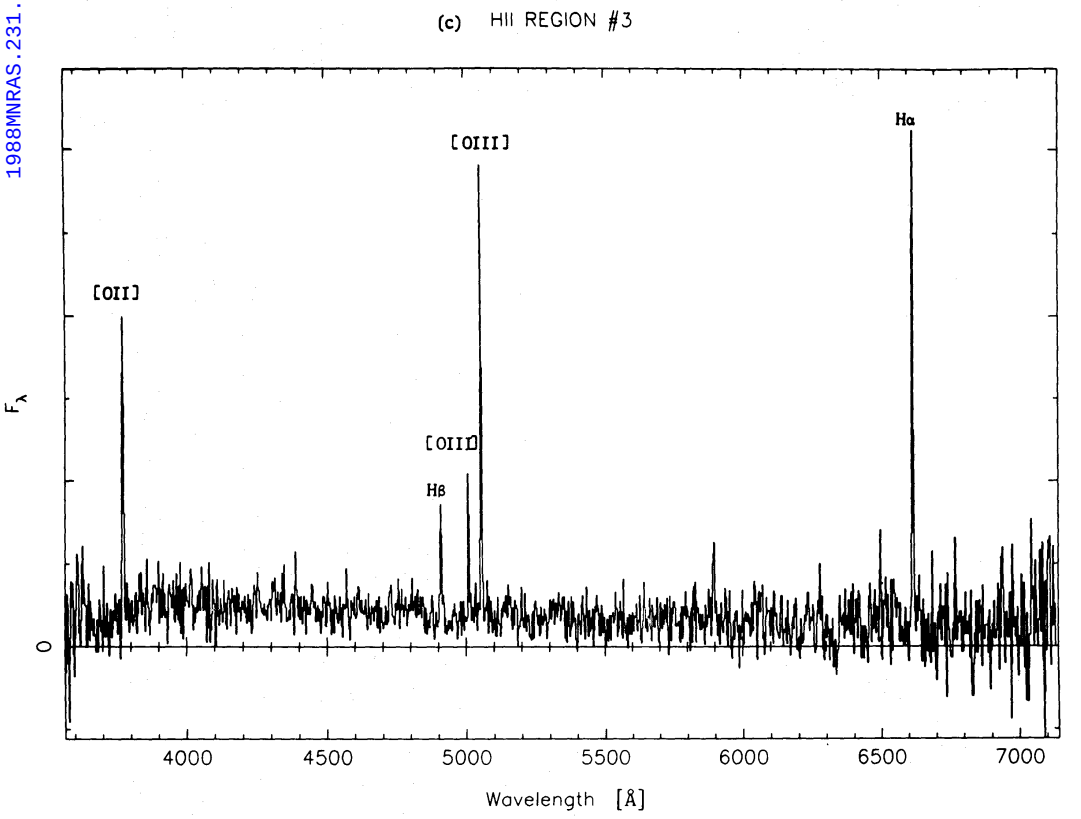

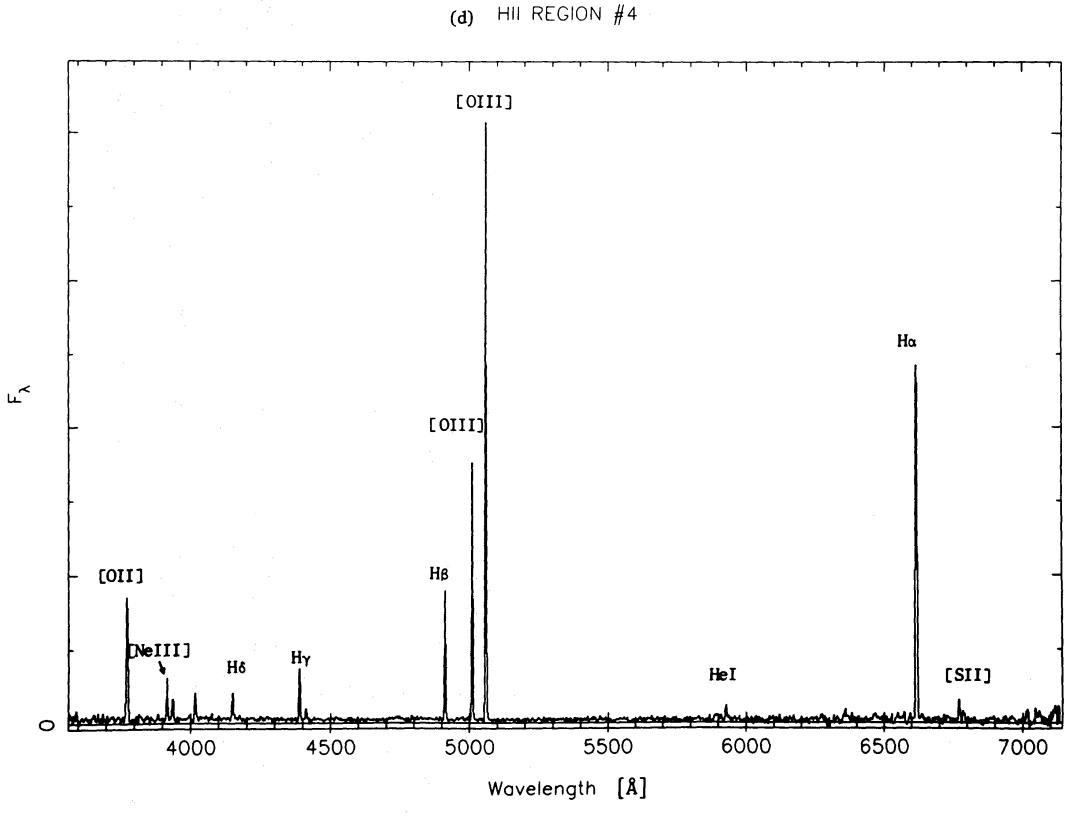

Figure 1–*continued*

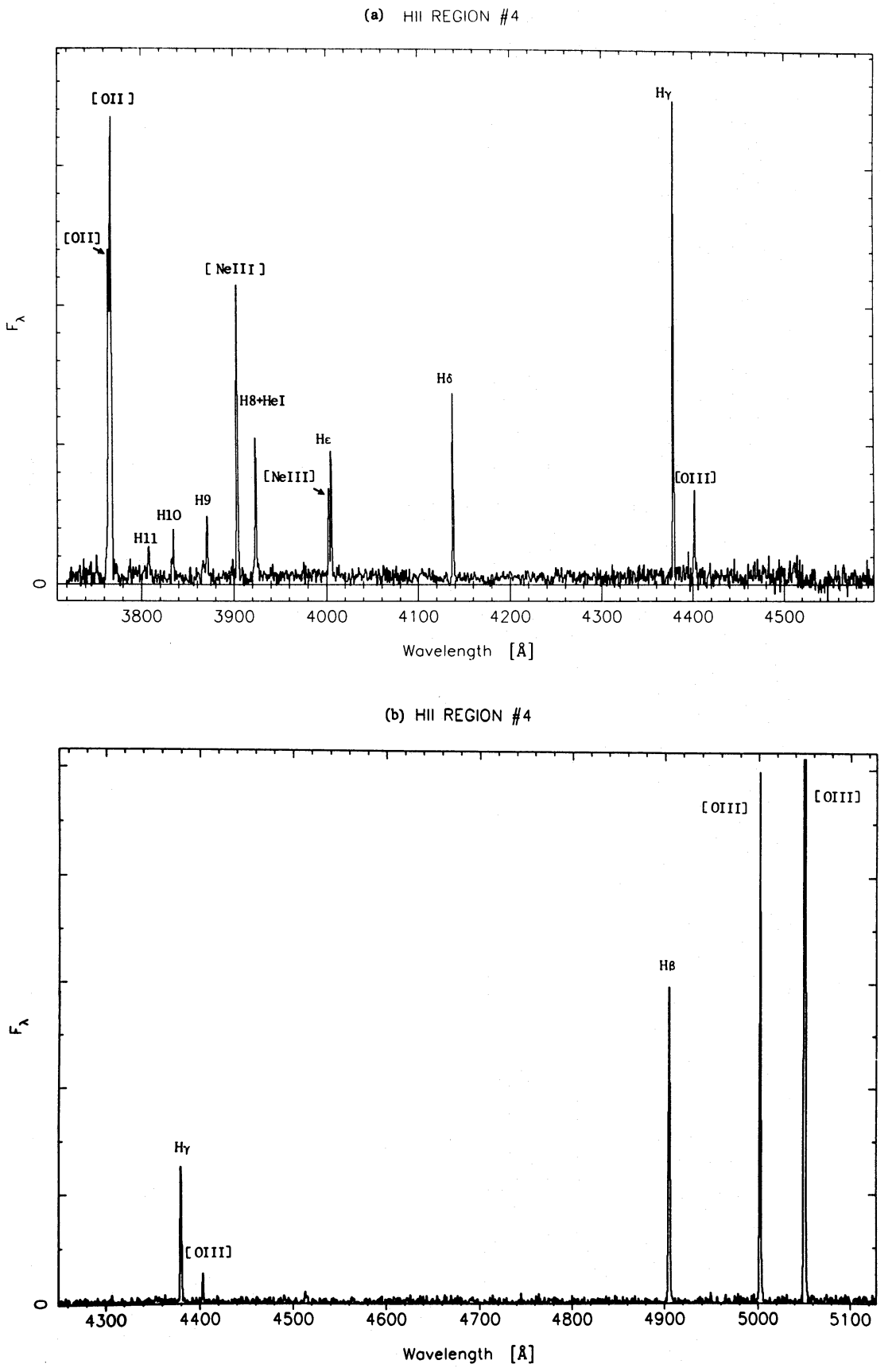

Figure 2. Intermediate-dispersion spectra (resolution 1.5 Å) of region 4 in the ultraviolet and blue wavebands. The redshifted [O III] λ5007 line is saturated. F_λ is the flux per Ångström (arbitrary units).

Table 2. Relative reddening-corrected line intensities for Michigan 160 (logarithmic relative to Hβ).

Line	Å	1	2	3	4
[OII]	3727	0.31±0.03	0.28±0.08	0.16±0.03	0.19±0.01
H11	3771	-	-	-	-1.14±0.18
H10	3798	-	-0.79±0.3	-	-1.09±0.17
H9	3835	-	-	-	-0.95±0.12
[NeIII]	3869	-0.42±0.09	-	-0.44±0.09	-0.43±0.03
H8+HeI	3889	-0.68±0.15	-	-0.94±0.41	-0.74±0.08
[NeIII]	3967	-1.03±0.01	-	-	-0.90±0.11
Hε	3970	-0.81±0.20	-	-0.66±0.3	-0.75±0.08
Hδ	4101	-0.62±0.13	-	-0.64±0.15	-0.65±0.06
Hγ	4340	-0.25±0.03	-0.43±0.27	-0.35±0.05	-0.37±0.03
[OIII]	4363	-1.26±0.26	-	-	-1.14±0.13
HeI	4471	<-1.40	-	-1.21±0.25	-1.32±0.3
Hβ	4861	0.00±0.02	0.00±0.06	0.00±0.02	0.00±0.02
[OIII]	4959	0.13±0.01	0.09±0.05	0.12±0.01	0.21±0.01
[OIII]	5007	0.56±0.01	0.57±0.02	0.59±0.01	0.69±0.01
HeI	5875	-1.40	-	-0.83±0.3	-0.72±0.12
[OI]	6300	<-1.52±0.3	<0.95±0.26	<-1.13±0.3	<-1.19±0.2
Hα	6563	0.46±0.04	0.46±0.04	0.43±0.07	0.46±0.01
[NII]	6584	<-0.8±0.3	<0.77±0.26	-1.13:±0.3	-1.31±0.3
[SII]	6725	<-1.4±0.3	-0.31±0.26	<-1.40	-0.64±0.3
E(B-V)		0.24	0.18	0.07	0.27
F(Hβ) 10^{-15}erg s^{-1}cm^{-2}		7.6	0.98	0.34	5.0
W(Hβ) Å		53±10	31±10	52±4	50±10
log L(Hβ) erg s^{-1}		39.48	38.59	38.13	39.29
V_{hel} km s^{-1}		2656±10	2704±5	2690±5	2646±5
σ (km s^{-1})		18±2	14±4	17±3	11±3

of 3 hr is shown in Fig. 3 and the observed H I parameters are listed in Table 3. A position–velocity map was also made using observations taken on a square grid of 3×3 points around the galaxy. A grid spacing of 6 arcmin was used and each position was observed for 40 min. We were able to trace the positional centroid of the H I emission from a velocity of 2656–2761 km s^{-1} using a boxcar resolution of 16 km $^{-1}$. There is a gradual increase of velocity from west to east in the galaxy, with a maximum separation of positional centroids at the extreme velocities of 2.0±0.5 arcmin at p.a. 80±35° (Table 3). The extent and p.a. of the line-of-centroids are in good agreement with the optical extent in Plate 1(b).

3 Temperatures and abundances

The observed intensity ratio of [O II] λλ3729/3726 is close to the lower limit of its sensitivity range for electron density (n_e), indicating a value for n_e of around 200 cm^{-3}. The electron temperatures

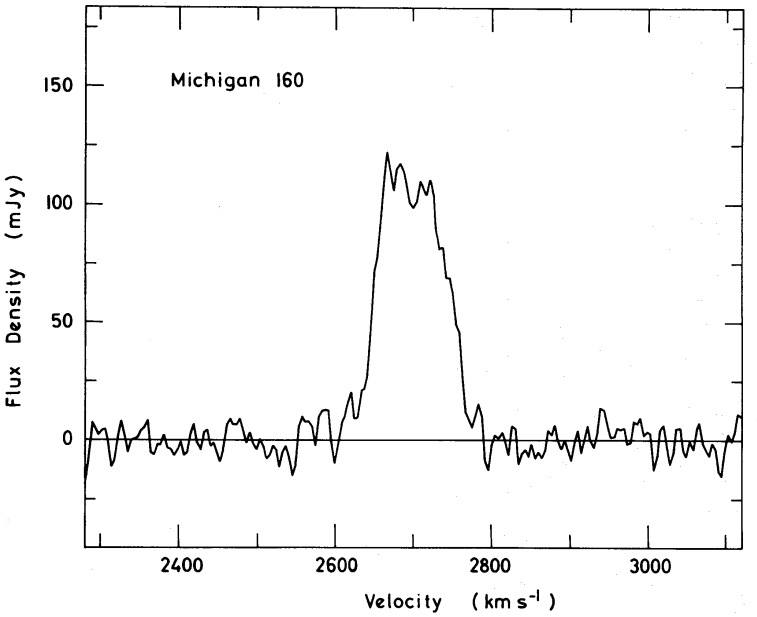

Figure 3. HI spectrum taken with the 76-m Lovell Telescope at Jodrell Bank. Integration time is 3 hr and the velocity resolution is 7 km s^{-1}.

Table 3. Neutral hydrogen results for Michigan 160.

Right Ascension(1) (1950)	$23^h21^m49^s$
Declination(2) (1950)	$-00°23'01''$
(i) *Observed Properties*	
Velocity, V_{50} ($c\Delta\lambda/\lambda_o$)	2700±4 km s^{-1}
Velocity width, W_{50}(2)	103±8 km s^{-1}
Velocity width, W_{20}(2)	132±10 km s^{-1}
Flux integral	11.6±1.1 Jy km s^{-1}
Dynamical HI diameter	2.0±0.5 arcmin
Dynamical position angle	80±35°
(ii) *Derived Properties*	
Distance(3)	57.3 h_{50}^{-1} Mpc
Neutral hydrogen mass, M_{HI}	8.97±0.90 x 10^9 h_{50}^{-2} $M_\odot$
Total mass (i=50°)	1.70±0.43 x 10^{10} h_{50}^{-1} $M_\odot$
HI fraction	53±14 h_{50}^{-1} per cent

(1) Optical position of region 1

(2) 50 and 20 per cent velocity widths in galaxy rest frame.

(3) h_{50} = 1 corresponds to H_o=50 km s^{-1} Mpc^{-1}. Distance allows for solar motion of 300 km s^{-1} to ℓ = 90°, b = 0°.

Table 4. Abundances.

	1	2	3	4
$12+\log(O^{++}/H^{+})$	7.73±0.3	7.73	7.75	7.85±0.15
$12+\log(O^{+}/H^{+})$	7.46±0.36	7.43	7.31	7.34±0.19
12+log(O/H)	7.92	7.91	7.89	7.97
log (O/N)	-	-	1.46:	-
log (O/Ne)	0.58	-	0.60	0.60
$O^{++}/(O^{++}+O^{+})$	0.65	0.67	0.73	0.76
Z	0.0022	0.0021	0.0020	0.0025

(T_e) in regions 1 and 4 were calculated using the observed [O III] line ratios and the collision strengths given by Seaton (1975). With our quoted errors on the [O III] λ4363 intensity, the values obtained for T_e are

$T_e(1)=13\,100\pm3400$ K

$T_e(4)=13\,000\pm1700$ K.

Although [O III] λ4363 was not detected in regions 2 and 3 the same temperature has been assumed. Ionic abundances for O^{2+}, O^{+} and Ne^{2+} have been derived using the atomic parameters referenced by Pagel *et al.* (1978) and assuming a uniform temperature along the line-of-sight ($t^2=0.0$). The conversion to total abundances given in Table 4 makes use of the standard ionization corrections also given by those authors. There is only one, marginal, detection of the [N II] λ6584 line and this gives at least an upper limit to the nitrogen abundance. The errors on $\log(O^{2+}/H^{+})$ and $\log(O^{+}/H^{+})$ in the table simply represent the uncertainty in the electron temperature given above. The abundance of helium is uncertain, as the errors inherent in the helium line strengths in our data make it strongly dependent on the weighting given to each of the lines. We shall therefore not discuss the abundance of helium in detail in this paper but note that in Michigan 160 it is broadly similar to that obtained for other IEHRs (Lequeux *et al.* 1979). The results for sulphur are similarly uncertain and are also not given in Table 4.

Total mass and neutral hydrogen fraction

Fig. 3 shows that Michigan 160 is bright in H I with a velocity width rather higher than observed for IZw18 (Lequeux & Viallefond 1980) but similar to that of IIZw40 (Fisher & Tully 1981). The broad flat-topped profile and the large H I velocity gradient observed across the galaxy indicates that there exists substantial rotation. It is therefore possible to estimate a total mass using the diameter equivalent to the line-of-centroids diameter ($33\pm8\,h_{50}^{-1}$ kpc) and a galaxy rotation at this diameter equal to one-half of the corresponding velocity difference (52 km s^{-1}). The total mass (assuming that it is spherically symmetric) is

$$M_T=1.00\pm0.25\times10^{10}h_{50}^{-1}\,\mathrm{cosec}^2 i\,M_\odot,$$

where i is the inclination angle of the galaxy from face-on. The neutral hydrogen mass of Michigan 160 derived from the integrated H I flux and distance in Table 3 is

$$M_{HI}=8.97\pm0.90\times10^{9}h_{50}^{-2}M_\odot$$

and the corresponding neutral hydrogen to total mass ratio is

$$M_{HI}/M_T=0.90\pm0.24\,\mathrm{cosec}^{-2} i\,h_{50}^{-1}.$$

Table 5. H II region mass calculations.

	HII REGION 1	2	3	4	α(1)	t(10^7yr)(2)
UV flux Q(H^0) (photons s^{-1})	6.2×10^{51}	8.0×10^{50}	2.8×10^{50}	4.1×10^{51}		
Equivalent number of O5 stars(3)	120	16	5	80		
Equivalent number of O7 stars(3)	860	110	39	570		
Mass($M_\odot$)(4) Model D	3.1×10^6	4.0×10^5	1.4×10^5	2.0×10^6	α=2	5
E	1.3×10^7	1.7×10^6	5.9×10^5	8.6×10^6	α=3	5
F	5.0×10^6	6.4×10^5	2.2×10^5	3.3×10^6	α=2	16
G	5.3×10^5	6.9×10^4	8.6×10^5	3.5×10^5	α=2	3
M_{HII}(virial)(5)	4.5×10^6	1.3×10^6	3.6×10^6	6.0×10^5		

(1) Slope of initial mass function.

(2) Age of starburst.

(3) Based on main-sequence fluxes in table 5.3 of Spitzer (1978).

(4) Mass of radiating stars based on the models used in Rieke *et al.* (1980).

(5) *c.f.* NGC 5253 8.8, LMC I 7.9, SMC I 0.76, IIZw40 35 and NGC 604 7.8×10^6 $M_\odot$ (Terlevich & Melnick 1981).

An estimate of the inclination angle (i) may be obtained from the apparent axial ratio (0.6) of the optical extent in Plate 1(b). This gives $i\approx50°$ and implies a neutral hydrogen-to-total mass ratio of ~53 per cent. This is an order of magnitude higher than the mean value for Sb/Sbc galaxies (Staveley-Smith & Davies 1987) of 5 per cent (for $H_0=50\,\mathrm{km\,s^{-1}\,Mpc^{-1}}$). Michigan 160 is therefore extremely rich in H I and, allowing for helium, would appear to have a total neutral gas fraction close to 70 per cent. In this context, it is interesting to note that existing H I observations of both giant and dwarf irregular galaxies also show a large gas-to-total mass ratio (Hunter & Gallagher 1985). The neutral hydrogen is not confined to the optical dimensions of such galaxies; for example, NGC 4449 (van Woerden, Bosma & Mebold 1975) appears to have H I at five times the Holmberg radius.

5 Discussion

5.1 THE MASSES OF THE H II REGIONS

With our limited data, it is not possible to construct detailed star formation histories (Huchra 1977; Gallagher, Hunter & Tutukov 1984) for the H II regions in Michigan 160. We can, however, crudely estimate the total mass of stars involved from the Hβ luminosity. Assuming Case B recombination, the number of ionizing ultraviolet photons required for each Hβ photon can be calculated from the relationships given by Osterbrock (1974) and the values of $\alpha_{\rm eff}$ and $\alpha_{\rm total}$ given in his tables 4.4 and 2.1 respectively. The total ultraviolet flux from each H II region $Q(H^0)$ is listed in Table 5 and is compared with the corresponding number of O stars required to produce this flux. Derivation of the total mass of stars involved requires knowledge of the form of the Initial Mass Function (IMF) and the evolutionary status of the burst. We have therefore used the starbust models presented by Rieke *et al.* (1980) to estimate a range of plausible stellar masses by

scaling to our values of $Q(H^0)$. Table 5 gives mass estimates derived by these methods. The masses vary between 10^5 and $10^7 M_\odot$ for the four H II regions, depending on the slope of the IMF and the age of the starburst. Each of the regions in Michigan 160 is therefore roughly equivalent in mass to 30 Doradus in the LMC.

Melnick *et al.* (1987) quote a relationship between Hβ luminosity [L(Hβ), in erg s^{-1}] and velocity dispersion (σ, in km s^{-1}) for giant H II regions of

$$\log L(\mathrm{H}\beta) = 4.2 \log \sigma + 34.1. \quad (1)$$

For the dispersions in Table 2, the agreement between the average observed and the average predicted Hβ luminosities for the four H II regions is reasonable, albeit with a large rms scatter (~2 mag) some of which is due to absorption. The remarkable closeness between this relationship and the well-known correlation between velocity dispersion and luminosity in elliptical galaxies (Faber & Jackson 1976) implies that H II regions are similarly gravitationally bound complexes whose linewidth reflects the random motions of the gas in the potential well of the gas and stars. A second estimate of the mass of the H II regions may thus be obtained from the observed velocity dispersion, using the semi-empirical relationship derived for giant H II regions (Terlevich & Melnick 1981; Melnick *et al.* 1987)

$$\log M_{\mathrm{H\,II}}/M_\odot = 4.6 \log \sigma + 0.9. \quad (2)$$

These mass estimates are given for each H II region in Table 5 and are in broad agreement with our previous estimates (~$10^6 M_\odot$). The total mass of the four H II regions in Michigan 160 is therefore approximately 0.1 per cent of the total galaxy mass.

5.2 THE EVOLUTIONARY STATUS OF MICHIGAN 160

From Table 4, it is clear that like other IEHRs the metal abundances of Michigan 160 are very low, and in fact fall close to those of the Small Magellanic Cloud, as its position on the log (N/O) versus log (O/H) plot for extragalactic H II regions illustrates (Fig. 4). The O/H abundance ratio appears to be typical of emission-line galaxies (Kunth & Sargent 1986). The Ne/O ratio (Table 4)

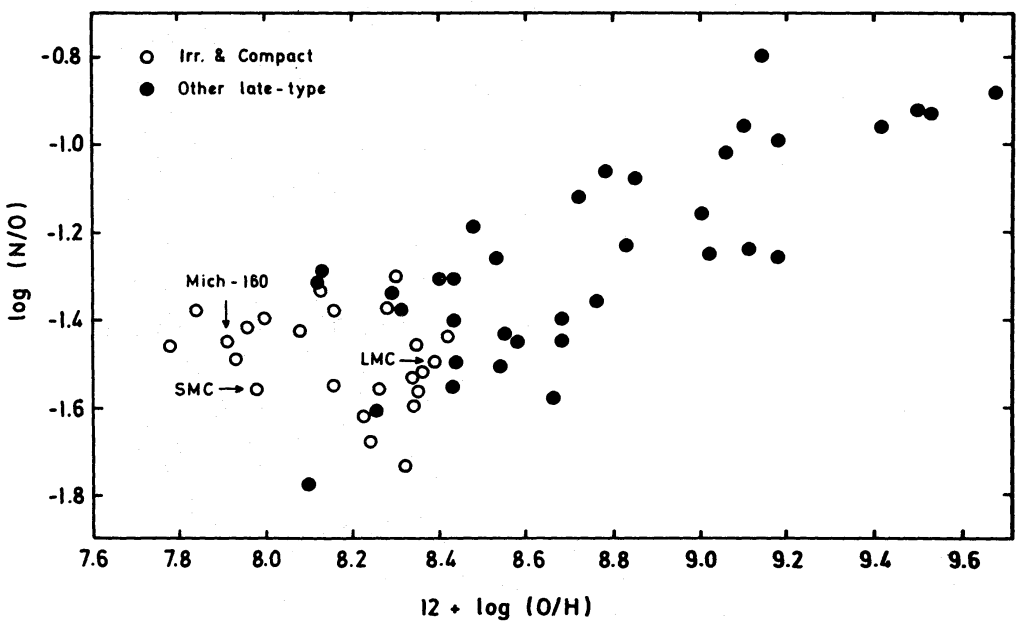

Figure 4. Relation between log (N/O) and log (O/H) for Michigan 160 and the extragalactic H II regions in the compilation of Pagel & Edmunds (1981).

fits in well with the general statement made by French (1980) that it is nearly constant in all objects, implying a common nucleosynthetic origin for these two elements (Vigroux, Stasińska & Comte 1987).

An interesting aspect of the results for Michigan 160 is the apparent lack of any abundance gradient (over a projected distance of 10 kpc) compared with large spiral galaxies. Pagel *et al.* (1978) suggest that, in the case of the SMC, this is a consequence of streaming motions associated with its bar. Although the H I data indicate that such a large-scale velocity field may exist in Michigan 160, there is no appreciable velocity gradient along the H II regions. These results can be reconciled provided that the H I is predominantly located away from the H II regions in a part of the galaxy with a substantially larger velocity field, which will exist, for example, if there is a slowly rising rotation curve or a large-scale warp. An alternative to streaming is that inflow of this unprocessed neutral gas is slowing down the enrichment process (Chiosi 1980; Matteucci & Chiosi 1983). This idea is particularly attractive in the light of recent work on the filamentary system surrounding NGC 5253, by one of us (DJA). Although gas accretion is not an efficient process for low-mass galaxies, it is nevertheless able to produce the low metallicities observed in relatively gas-poor blue compact galaxies such as IZw18 and Mkn 36. The relation between metallicity (z) and neutral gas fraction (M_g/M_T) in a system where stellar mass loss and infall are balanced by star formation is

$$z=p\,[1-\exp(1-M_T/M_g)] \tag{3}$$

for a constant heavy element yield p (e.g. Tinsley 1980), the metallicity being related to the oxygen abundance by $z\approx 25\,(O/H)$. In Fig. 5, we plot the oxygen abundance for Michigan 160 and a sample of 39 emission-line and late-type galaxies as a function of total-to-neutral mass ratio. Apart from Michigan 160, the data used are from the compilation of Matteucci & Chiosi (1983) and scaled to $H_0=50\,\mathrm{km\,s^{-1}\,Mpc^{-1}}$. Helium content has been allowed for by assuming that the total neutral gas mass is 1.3 times the H I mass (Lequeux *et al.* 1979). Michigan 160 is amongst the most gas-rich and metal-poor galaxies and lies close to a line of constant yield ($p=0.004$) defined by equation (3). Also plotted (dashed line) is the metallicity-dependent yield model by Peimbert

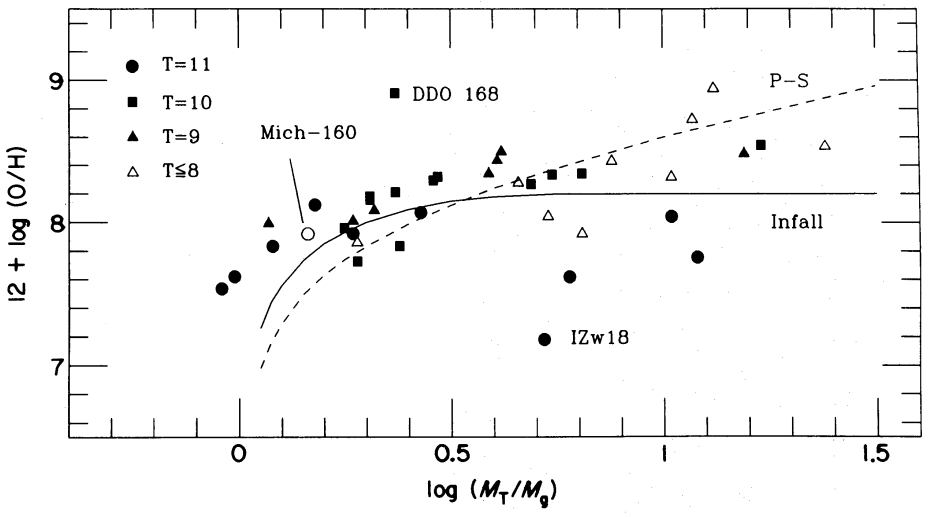

Figure 5. Oxygen abundance [12+log (O/H)] versus the logarithm of the total-to-neutral mass ratio for H II regions in late-type galaxies. Blue compact galaxies are classified as $T=11$, irregulars as $T=10$ and spiral/magellanics as $T=9$. The solid curve is the infall model described in the text ($p=0.004$). The dashed line refers to the variable yield model of Peimbert & Serrano (1982). The two unphysical points with $M_g>M_T$ are a result of measurement and distance uncertainties.

& Serrano (1982) for a single-zone system (no inflow or outflow). At this stage, the uncertainties in some of the observational data plotted in Fig. 5 are large, particularly for the total mass M_T. We note, however, that the Peimbert–Serrano metallicity-dependent yield model which is successful for evolved H II regions (Edmunds & Pagel 1984) appears to underestimate the oxygen abundance of the gas-rich galaxies plotted in Fig. 5, and overestimate the abundance for gas-poor galaxies. The straightforward infall model with constant yield ($p=0.004$) is a more satisfactory fit to the data.

The disturbed structure of the outer parts of Michigan 160 (Plate 1b) raises the possibility that some form of interaction has triggered the process of massive star formation. French (1980) has noted that all the high-luminosity [$L(\mathrm{H}\beta) > 10^{41}\,\mathrm{erg\,s^{-1}}$] IEHR systems have associated companion galaxies suggesting that a tidal interaction is responsible. Baldwin, Spinrad & Terlevich (1982) have reported optical observations of IIZw40 which suggest that the star burst occurring in this system is a consequence of a tidal interaction between two merging galaxies. Terlevich (private communication) has found similar morphological evidence for many other low-luminosity IEHRs. In this context it would seem appropriate to determine the redshift of the dwarf companion 80 arcsec north of Michigan 160 (Plate 1b) which we regard as a candidate interactor.

6 Conclusions

The emission-line galaxy Michigan 160 has been shown to be a relatively young and unevolved system currently undergoing a burst of star formation. Spectrophotometry of the four bright H II regions show its heavy element abundance to be similar to those of the SMC and other emission-line and compact galaxies. The H II regions in Michigan 160 are particularly luminous. Both their internal velocity dispersion and their Hβ luminosity demonstrate that they are likely to be as massive as 30 Doradus. Neutral hydrogen observations show that Michigan 160 is even more remarkable, being amongst the most gas-rich galaxies known. The large H I linewidth and the east–west velocity gradient probably imply an outer rotation velocity of 50 km s^{-1} in projection. In order to reconcile this result with the small velocity gradient found across the H II regions, we suggest that the H I is distributed at a larger radius, with a slowly rising rotation curve or a large-scale warp in the galaxy. Interferometric observations in H I would help clarify this point.

We have proposed that inflow from the unprocessed gaseous halo may be responsible for the low metal abundances and that a recent interaction, possibly with its dwarf companion, has triggered the current wave of star formation.

Acknowledgments

We thank David Malin for his photographic enhancement of the plate of Michigan 160.

References

Axon, D. J. & Taylor, K., 1984. *Mon. Not. R. astr. Soc.*, **207,** 241.
Baldwin, J. A., Spinrad, H. & Terlevich, R., 1982. *Mon. Not. R. astr. Soc.*, **198,** 535.
Boksenberg, A., 1972. In: *Auxiliary Instrumentation for Large Telescopes, Proc. ESO-CERN Conf.*, p. 295, eds Lausten, S. & Reiz, A., Geneva.
Brocklehurst, M., 1971. *Mon. Not. R. astr. Soc.*, **153,** 471.
Chiosi, C., 1980. *Astr. Astrophys.*, **83,** 206.
Davidson, K. & Kinman, T. D., 1985. *Astrophys. J. Suppl.*, **58,** 321.
Edmunds, M. G. & Pagel, B. E. J., 1984. *Mon. Not. R. astr. Soc.*, **211,** 507.
Faber, S. M. & Jackson, R. E., 1976. *Astrophys. J.*, **204,** 668.
Fisher, J. R. & Tully, R. B., 1981. *Astrophs. J. Suppl.*, **47,** 139.
French, H. B., 1980. *Astrophys. J.*, **240,** 41.

Gallagher, J. S., Hunter, D. A. & Tutukov, A. V., 1984. *Astrophys. J.,* **284,** 544.
Gondhalekar, P. M., Morgan, D. H., Dopita, M. & Phillips, A. P., 1984. *Mon. Not. R. astr. Soc.,* **209,** 59.
Huchra, J. P., 1977. *Astrophys. J.,* **217,** 928.
Hunter, D. A. & Gallagher, J. S., 1985. *Astrophys. J. Suppl.,* **58,** 533.
Kunth, D. & Sargent, W. L. W., 1986. *Astrophys. J.,* **300,** 496.
Lequeux, J. & Viallefond, F., 1980. *Astr. Astrophys.,* **91,** 269.
Lequeux, J., Peimbert, M., Rayo, J. F., Serrano, A. & Torres-Peimbert, S., 1979. *Astr. Astrophys.,* **80,** 155.
MacAlpine, G. M., Smith, S. B. & Lewis, D. W., 1977. *Astrophys. J. Suppl.,* **35,** 197.
Matteucci, F. & Chiosi, C., 1983. *Astr. Astrophys.,* **123,**121.
Melnick, J., Moles, M., Terlevich, R. & Garcia-Pelayo, J-M., 1987. *Mon. Not. R. astr. Soc.,* **226,** 849.
Oke, J. B., 1974. *Astrophys. J. Suppl.,* **27,** 21.
Osterbrock, D. E., 1974. *Astrophysics of Gaseous Nebulae,* San Francisco, Freeman.
Pagel, B. E. J. & Edmunds, M. G., 1981. *Ann. Rev. Astr. Astrophys.,* **19,** 77.
Pagel, B. E. J., Edmunds, M. G., Foxbury, R. A. E. & Webster, B. L., 1978. *Mon. Not. R. astr. Soc.,* **184,** 569.
Peimbert, M. & Serrano, A., 1982. *Mon. Not. R. astr. Soc.,* **198,** 563.
Rieke, G. H., Lebofsky, M. J., Thompson, R. I., Low, F. J. & Tokunaga, A. T., 1980. *Astrophys. J.,* **238,** 24.
Sargent, W. L. W. & Searle, L., 1970. *Astrophys. J.,* **162,** L155.
Seaton, M. J., 1975. *Mon. Not. R. astr. Soc.,* **170,** 475.
Spitzer, L., 1978. *Physical Processes in the Interstellar Medium,* Wiley, New York.
Staveley-Smith, L. & Davies, R. D., 1987. *Mon. Not. R. astr. Soc.,* **224,** 953.
Terlevich, R. & Melnick, J., 1981. *Mon. Not. R. astr. Soc.,* **195,** 839.
Thuan, T. X., 1983. *Astrophys. J.,* **268,** 667.
Tinsley, B. M., 1980. *Fundamentals of Cosmic Physics,* **5,** 287.
van Woerden, H., Bosma, A. & Mebold, U., 1975. In: *La Dynamique des Galaxies Spirales,* p. 483, CNRS, Paris.
Vigroux, L., Stasińska, G. & Comte, G., 1987. *Astr. Astrophys.,* **172,** 15.
Whitford, A. E., 1958. *Astr. J.,* **63,** 201.